

1 Measurement of medium-induced modification of jet yield  
2 and acoplanarity using semi-inclusive  $\gamma_{\text{dir}}+\text{jet}$  and  $\pi^0+\text{jet}$   
3 distributions in  $p+p$  and central Au+Au collisions at  
4  $\sqrt{s_{NN}} = 200$  GeV by STAR\*

5 DEREK ANDERSON (FOR THE STAR COLLABORATION)

6 Cyclotron Institute, Texas A&M University, College Station, TX 77843

7 *Received August 11, 2022*

8 The STAR collaboration presents measurements of semi-inclusive dis-  
9 tributions of charged jets recoiling from high transverse energy ( $E_T$ ) direct  
10 photon and  $\pi^0$  triggers in  $p+p$  and central Au+Au collisions at  $\sqrt{s_{NN}} = 200$   
11 GeV. Jets are reconstructed from charged particles using the anti- $k_T$  algo-  
12 rithm with jet resolution parameters  $R = 0.2$  and  $0.5$ . The large un-  
13 correlated background in central Au+Au collisions is corrected using a  
14 mixed-event technique. This enables a jet measurement extending to low  
15 transverse momentum and large  $R$  with well-controlled systematic uncer-  
16 tainties. We present measurements of the jet  $R$  dependence of suppression,  
17 intra-jet broadening, and acoplanarity of  $\pi^0+\text{jet}$  and  $\gamma_{\text{dir}}+\text{jet}$  for trigger  
18  $E_T$  ( $E_T^{\text{trig}}$ ) between 9 – 20 GeV.

19 **1. Introduction**

20 Heavy-ion collisions at RHIC and the LHC produce a medium of decon-  
21 fined partons, the Quark-Gluon Plasma (QGP) [1]. Hard (high momentum  
22 transfer,  $Q^2$ ) interactions of quarks and gluons in such collisions generate en-  
23 ergetic scattered partons which propagate through the medium and interact  
24 with it. Consequently, the parton showers are modified (jet quenching) [2].  
25 Jet quenching manifests in several observable effects: transport of energy  
26 outside of the reconstructed jet cone, modification of the jet substructure,  
27 and enhanced acoplanarity ( $\Delta\phi = \phi_{\text{trig}} - \phi_{\text{jet}}$ ) [4]. While the  $\Delta\phi$  distribu-  
28 tion has a finite width in vacuum due to Sudakov radiation [3], the presence  
29 of a medium may further broaden it due to mechanisms such as multiple  
30 in-medium soft scatterings [4], the hard scattering of a parton off QGP  
31 quasi-particles [5], and medium response [6].

---

\* Presented at Quark Matter 2022

32 In these proceedings, the STAR collaboration reports measurements of  
 33 the semi-inclusive yields of jets recoiling from *direct photons* ( $\gamma_{\text{dir}}$ ) and  $\pi^0$ ,  
 34 together with their acoplanarity distributions in  $p+p$  and central Au+Au  
 35 collisions at  $\sqrt{s_{\text{NN}}} = 200$  GeV. Simultaneous measurements of these differ-  
 36 ent observables in the same analysis promise a discriminating and multi-  
 37 messenger approach to the study of jet quenching.

38 Since direct photons are color neutral, they do not interact with the  
 39 QGP; their measured energy thereby reflects the  $Q^2$  of the hard interaction  
 40 and provides a constraint on the initial energy of the recoiling jet. Hence,  
 41 the measurement of jets coincident with a  $\gamma_{\text{dir}}$  ( $\gamma_{\text{dir}}+\text{jet}$ ) provides a valuable  
 42 tool for quantifying the effects of jet quenching [7]. In addition, compar-  
 43 ison with jets coincident with  $\pi^0$  ( $\pi^0+\text{jet}$ ) may elucidate the color factor  
 44 and path length dependence of medium-induced energy loss, due to differ-  
 45 ences between the recoil jet populations of the two triggers in their relative  
 46 quark/gluon fraction and mean path length [8].

47 STAR has previously reported the yield suppression of charged hadrons  
 48 coincident with  $\pi^0$  and  $\gamma_{\text{dir}}$  triggers [9]. Additionally, STAR has measured  
 49 the yield of reconstructed charged-particle jets coincident with charged  
 50 hadron triggers ( $h^\pm+\text{jet}$ ) using a semi-inclusive approach [10]. In this ap-  
 51 proach, the large uncorrelated jet background in heavy-ion collisions is cor-  
 52 rected with a Mixed Event (ME) technique, enabling the measurement of  
 53 reconstructed jets at low transverse momentum ( $p_{\text{T}}$ ) and large resolution  
 54 parameter. In the current analysis, we combine the  $\gamma_{\text{dir}}/\pi^0$  identification of  
 55 [9] with the semi-inclusive and ME approach of [10] to measure the semi-  
 56 inclusive  $\gamma_{\text{dir}}+\text{jet}$  and  $\pi^0+\text{jet}$  yields in  $p+p$  and central Au+Au collisions.

## 57 2. Analysis

58 Two STAR datasets of  $\sqrt{s_{\text{NN}}} = 200$  GeV collisions are analyzed: a  
 59  $10 \text{ nb}^{-1}$  sample of Au+Au collisions recorded in 2014, and a  $23 \text{ pb}^{-1}$  sample  
 60 of  $p+p$  collisions recorded in 2009. Both were recorded using an online high  
 61 tower trigger, i.e. a calorimeter tower above a certain threshold in energy.  
 62 Two STAR subsystems are used: the Time Projection Chamber (TPC) [11],  
 63 which provides charged-particle tracks for jet reconstruction, and the Barrel  
 64 Electromagnetic Calorimeter (BEMC) [12], which is used to identify  $\pi^0$  and  
 65  $\gamma_{\text{dir}}$  triggers.

66 Discrimination of  $\pi^0$  and  $\gamma_{\text{dir}}$  candidates in the BEMC is carried out  
 67 using the Transverse Shower Profile (TSP) method [9, 13]. Based on the  
 68 TSP, the data are separated into two samples: a nearly pure sample of  
 69 identified  $\pi^0$ , and a sample with an enhanced fraction of  $\gamma_{\text{dir}}$  ( $\gamma_{\text{rich}}$ ).

70 Triggers are selected offline to satisfy  $E_{\text{T}}^{\text{trig}} = 9-20$  GeV and  $|\eta^{\text{trig}}| < 0.9$ .  
 71 The purity of the  $\gamma_{\text{rich}}$  sample, i.e., the percentage of  $\gamma_{\text{rich}}$  that are actually

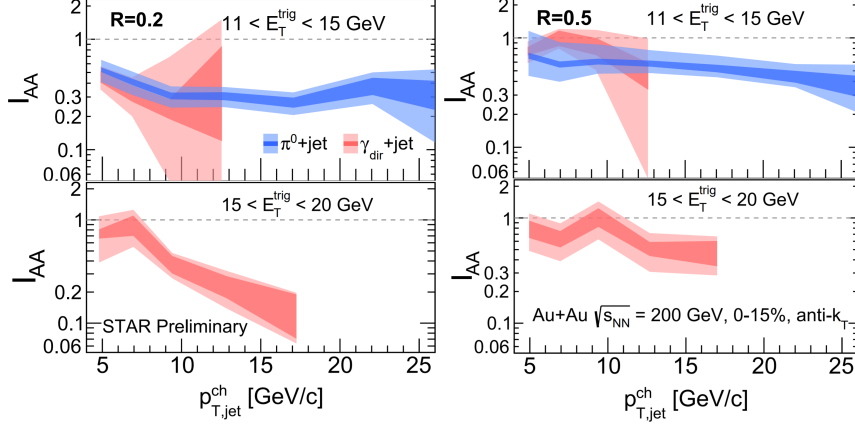


Fig. 1:  $I_{AA}$  for  $\pi^0$ +jet (blue) and  $\gamma_{\text{dir}}$ +jet (red). Dark bands indicate statistical errors, and light bands indicate systematic uncertainties.

72  $\gamma_{\text{dir}}$ , is determined via a data driven method [9, 13]. The  $\gamma_{\text{dir}}$ +jet distribu-  
 73 tion is then determined from the  $\gamma_{\text{rich}}$  sample via a statistical subtraction,  
 74 which removes contamination due to hadronic decays and fragmentation  
 75 photons to the extent that their near-side azimuthal correlations are identi-  
 76 cal to those of the identified  $\pi^0$  [9, 13].

77 Jets are reconstructed from the TPC tracks using the anti- $k_T$  algorithm  
 78 [14, 15] for two resolution parameters,  $R = 0.2$  and  $0.5$ . Reconstructed jets  
 79 are subjected to the same fiducial cuts as in [10].

80 In Au+Au collisions, there is a substantial background yield of jet candi-  
 81 dates which are not correlated with the trigger. This background yield is  
 82 removed using the ME technique described in [10]. Uncorrelated jet yield  
 83 is small in  $p+p$  collisions, and no correction for it is applied. The residual  
 84 jet  $p_T$ -smearing is corrected in two steps [10]: first, jets are corrected for  
 85 an event-wise energy pedestal, and then residual fluctuations caused by de-  
 86 tector effects ( $p+p$  and Au+Au collisions) and the heavy-ion background  
 87 (Au+Au collisions only) are corrected using regularized unfolding. We use  
 88  $p_{T,\text{jet}}^{\text{reco,ch}}$  (where the superscript “ch” denotes “charged jets”) to refer to the  
 89 jet  $p_T$  after the event-wise pedestal correction, and  $p_{T,\text{jet}}^{\text{ch}}$  to the jet  $p_T$  after  
 90 unfolding.

91 The two-dimensional acoplanarity distributions must also be unfolded  
 92 for both  $p_{T,\text{jet}}^{\text{reco,ch}}$  and  $\Delta\phi$  fluctuations. Note that the  $\Delta\phi$  distributions shown  
 93 here have however been unfolded for  $p_{T,\text{jet}}^{\text{reco,ch}}$  fluctuations only. We estimate  
 94 that  $\Delta\phi$  smearing effects are small.

95

### 3. Results

96 Jet distributions are reported in two ways: the two-dimensional measure-  
 97 ment of  $\Delta\phi$  vs.  $p_{T,\text{jet}}^{\text{reco, ch}}$ , and the one-dimensional measurement of  $p_{T,\text{jet}}^{\text{reco, ch}}$   
 98 for recoil jets, which satisfy  $|\Delta\phi - \pi| < \pi/4$ . The recoil jet  $p_{T,\text{jet}}^{\text{ch}}$  distribu-  
 99 tions in central Au+Au and  $p+p$  are compared against PYTHIA-8 with the  
 100 MONASH tune [17]. The PYTHIA-8 distributions are smeared to account  
 101 for a trigger energy resolution (see the slides accompanying these proceed-  
 102 ings). We report two different ratios of the trigger-normalized recoil jet  
 103 yields:  $I_{AA}$ , the ratio of the semi-inclusive yield of recoil jets in Au+Au  
 104 over that in  $p+p$  for fixed  $R$ ; and  $\mathfrak{R}^{0.2/0.5}$ , the ratio of the semi-inclusive  
 105 yield for  $R = 0.2$  relative to that for  $R = 0.5$ , for fixed collision system.

106 Figure 1 shows  $I_{AA}$  for  $E_T^{\text{trig}} = 11 - 15, 15 - 20$  GeV  $\pi^0$  and  $\gamma_{\text{dir}}$  triggers.  
 107 The recoil jet yield for  $R = 0.2$  is systematically more suppressed than that  
 108 for  $R = 0.5$ . In addition, the value of  $I_{AA}$  is observed to be consistent within  
 109 uncertainties between  $\pi^0$  and  $\gamma_{\text{dir}}$  for both values of  $R$ , despite differences  
 110 in the recoil jet quark/gluon fraction and mean path length. Note, however,  
 111 that the  $\gamma_{\text{dir}}$ +jet  $p_{T,\text{jet}}^{\text{ch}}$  spectrum is steeper, so a similar magnitude of yield  
 112 suppression corresponds to smaller medium-induced out-of-cone energy loss.

113 Figure 2 shows the  $\mathfrak{R}^{0.2/0.5}$  for  
 114  $E_T^{\text{trig}} = 11 - 15$  GeV  $\pi^0$  (upper  
 115 panel) and  $E_T^{\text{trig}} = 15 - 20$  GeV  
 116  $\gamma_{\text{dir}}$  (lower panel). We see that  
 117  $\mathfrak{R}^{0.2/0.5}$  for  $p+p$  is less than unity  
 118 and that PYTHIA-8 reproduces the  
 119 ratio well. However, the value of  
 120  $\mathfrak{R}^{0.2/0.5}$  for central Au+Au is signifi-  
 121 cantly lower than that for  $p+p$  and  
 122 PYTHIA-8.

123 Figures 1 and 2 show a clear  
 124 observation of significant medium-  
 125 induced intra-jet broadening in cen-  
 126 tral Au+Au collisions at RHIC.

127 Figure 3a shows the corrected  
 128  $\Delta\phi$  correlations in  $p+p$  collisions  
 129 between  $E_T^{\text{trig}} = 9 - 11$  GeV  $\pi^0$   
 130 triggers and  $R = 0.5$  jets (boxes).  
 131 These distributions are reproduced  
 132 well by PYTHIA-8 (dotted lines) for all three ranges of  $p_{T,\text{jet}}^{\text{ch}}$  (5–10, 10–15,  
 133 and 15–20 GeV/c).

134 Figure 3b shows the corrected  $\Delta\phi$  correlations in Au+Au collisions  
 135 between  $E_T^{\text{trig}} = 11 - 15$  GeV  $\pi^0$  and  $\gamma_{\text{dir}}$  triggers and recoil jets of  $R = 0.5$

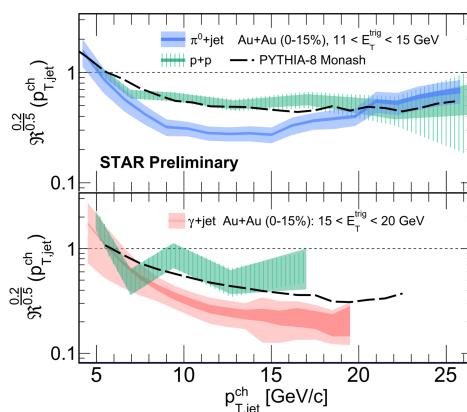


Fig. 2:  $\mathfrak{R}^{0.2/0.5}$  for  $\pi^0$  (upper panel) and  $\gamma_{\text{dir}}$  (lower panel) triggers from  $p+p$  (green), Au+Au (blue and red), and PYTHIA-8 (black dashed lines).

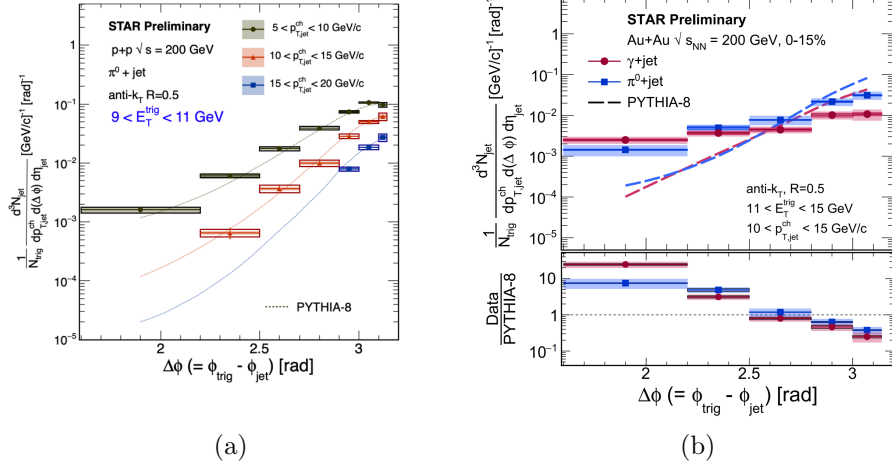


Fig. 3: Corrected  $R = 0.5$   $\Delta\phi$  distributions in  $p+p$  (a) and Au+Au (b) collisions for  $\pi^0$  ( $p+p$  and Au+Au) and  $\gamma_{\text{dir}}$  (Au+Au only) triggers. Vertical lines indicate statistical errors, and filled and open boxes indicate uncorrelated and correlated systematic uncertainties, respectively (note that the statistical errors are smaller than the marker size for the Au+Au data points). Dotted and dashed lines are PYTHIA-8.

136 and  $p_{T,\text{jet}}^{\text{ch}} = 10 - 15$  GeV/c. The dashed lines are the corresponding distri-  
 137 butions from PYTHIA-8, that is validated in the left panel. We observe a  
 138 marked enhancement in yield at wide angles (small  $\Delta\phi$ ) in central Au+Au  
 139 collisions relative to vacuum fragmentation. This is the first observation  
 140 of significant medium-induced modification of  $\pi^0$ +jet and  $\gamma_{\text{dir}}$ +jet acopla-  
 141 narity at low  $p_{T,\text{jet}}^{\text{ch}}$  in central Au+Au collisions at RHIC.

#### 142 4. Summary

143 STAR has measured the  $R$  dependence of recoil jet yield, and acopla-  
 144 narity using the semi-inclusive distributions of charged-particle jets recoiling  
 145 from  $\pi^0$  and  $\gamma_{\text{dir}}$  triggers in central Au+Au and  $p+p$  collisions at  $\sqrt{s_{\text{NN}}} =$   
 146 200 GeV. Model calculations based on the PYTHIA-8 event generator are  
 147 found to be consistent with the measurements in  $p+p$  collisions.

148 We have reported both the recoil yield in a fixed angular window as a  
 149 function of  $p_{T,\text{jet}}^{\text{ch}}$ , and the distribution of acoplanarity at fixed  $p_{T,\text{jet}}^{\text{ch}}$ . We  
 150 observe marked medium-induced intra-jet broadening. We also observe clear  
 151 medium-induced acoplanarity at low jet  $p_{T,\text{jet}}^{\text{ch}}$ , which may arise from in-  
 152 medium jet scattering or from the contribution of medium response to the  
 153 jet signal. To further investigate the medium-induced acoplanarity and

154 disentangle the underlying mechanisms, it will be essential to extend the  
155 kinematic range of this measurement in heavy-ion collisions and compare  
156 against theoretical calculations.

### 157 Acknowledgements

158 This work funded in part by the United States Department of Energy  
159 under grant number DE-SC0015636.

### REFERENCES

- 160 [1] W. Busza, K. Rajagopal, and W. van der Schee, *Ann. Rev. Nucl. Part. Sci.* **68**,  
161 339 (2018)
- 162 [2] L. Cunqueiro and A. M. Sickles, (2021) arXiv:2110.14490 [nucl-ex]
- 163 [3] P. Sun, C.-P. Yuan, and F. Yuan, *Phys. Rev. D* **92**, 094007 (2015)
- 164 [4] A. Mueller *et al.*, *Phys. Lett. B* **763**, 208 (2016)
- 165 [5] F. D'Eramo, M. Lekaveckas, H. Liu, and K. Rajagopal, *J. High Energy Phys.*  
166 **2005**, 031 (2005)
- 167 [6] G. Milhano, U. A. Wiedemann, and K. C. Zapp, *Phys. Lett. B* **779**, 409 (2018)
- 168 [7] X.-N. Wang, Z. Huang, and I. Sarcevic, *Phys. Rev. Lett.* **77**, 231 (1996)
- 169 [8] T. Renk, *PRC* **88**, 054902 (2013)
- 170 [9] L. Adamczyk *et al.*, *Phys. Lett. B* **760**, 689(2016)
- 171 [10] L. Adamczyk *et al.*, *Phys. Rev. C* **96**, 024905 (2017)
- 172 [11] M. Anderson *et al.*, *Nucl. Instrum. Methods Phys. Res., Sect. A* **499**, 659  
173 (2003)
- 174 [12] M. Beddo *et al.*, *Nucl. Instrum. Methods Phys. Res., Sect. A* **499**, 725 (2003)
- 175 [13] B. I. Abelev *et al.*, *Phys. Rev. C* **82**, 034909 (2010)
- 176 [14] M. Cacciari, G. P. Salam, and G. Soyez, *J. High Energy Phys.* **2008**, 063  
177 (2008)
- 178 [15] M. Cacciari, G. P. Salam, and G. Soyez, *Euro. Phys. J. C* **72**, 1896 (2012)
- 179 [16] T. Adye, (2011) arXiv:1105.1160 [physics.data-an]
- 180 [17] T. Sjöstrand, S. Mrenna, and P. Z. Skands, *Comput. Phys. Commun.* **178**,  
181 852 (2008)
- 182 [18] N.-B. Chang and G.-Y. Qin, *Phys. Rev. C* **94**, 024902 (2016)
- 183 [19] T. Luo, S. Cao, Y. He, and X.-N. Wang, *Phys. Lett. B* **782**, 707 (2018)
- 184 [20] M. D. Sievert, I. Vitev, and B. Yoon, *Phys. Lett. B* **795**, 502 (2019)